

NAVAL POSTGRADUATE SCHOOL Monterey, California



**Real-Time Tracking and Display of Human Limb
Segment Motions Using Sourceless Sensors
and a Quaternion-Based Filtering Algorithm –
Part II: Calibration and Implementation**

by

Eric R. Bachmann
Robert B. McGhee
Xiaoping Yun
Michael J. Zyda

May 2001

Approved for public release; distribution is unlimited.

Prepared for: NPS Moves Academic Group

REPORT DOCUMENTATION PAGE

Form approved
OMB No 0704-0188

Public reporting burden for this collection of information is estimated to average 1 hour per response, including the time for reviewing instructions, searching existing data sources, gathering and maintaining the data needed, and completing and reviewing the collection of information. Send comments regarding this burden estimate or any other aspect of this collection of information, including suggestions for reducing this burden, to Washington Headquarters Services, Directorate for Information Operations and Reports, 1215 Jefferson Davis Highway, Suite 1204, Arlington, VA 22202-4302, and to the Office of Management and Budget, Paperwork Reduction Project (0704-0188), Washington, DC 20503.

1. AGENCY USE ONLY (Leave blank)	2. REPORT DATE May 2001	3. REPORT TYPE AND DATES COVERED Technical Report
----------------------------------	----------------------------	--

4. TITLE AND SUBTITLE Real-Time Tracking and Display of Human Limb Segment Motions Using Sourceless Sensors and a Quaternion-Based Filtering Algorithm – Part I: Calibration and Implementation	5. FUNDING N6M ARO
--	---------------------------

6. AUTHOR(S) Bachmann, Eric R., McGhee, Robert B., Yun, Xiaoping, and Zyda, Michael J.

7. PERFORMING ORGANIZATION NAME(S) AND ADDRESS(ES) Naval Postgraduate School Monterey, CA 93943-5118	8. PERFORMING ORGANIZATION REPORT NUMBER NPS-MV-01-003
--	---

9. SPONSORING/MONITORING AGENCY NAME(S) AND ADDRESS(ES)	10. SPONSORING/MONITORING AGENCY REPORT NUMBER
---	--

11. SUPPLEMENTARY NOTES The views expressed in this thesis are those of the author and do not reflect the official policy or position of the Department of Defense or the U.S. Government.

12a. DISTRIBUTION/AVAILABILITY STATEMENT Approved for public release; distribution is unlimited.	12b. DISTRIBUTION CODE
---	------------------------

13. ABSTRACT (Maximum 200 words.)
Rigid body orientation may be determined without the aid of a generated source using a nine-axis MARG (Magnetic field, Angular Rate, and Gravity) sensor containing three orthogonally mounted rate sensors, three orthogonal linear accelerometers and three orthogonal magnetometers. Part I of this paper described a quaternion-based complementary filter algorithm for processing the output data from such a sensor. This paper focuses on the implementation of that theory. It describes a system designed to determine the posture of an articulated body in real-time. In the system the orientation of each segment relative to an Earth-fixed reference frame is individually determined through the use of an attached MARG sensor. The orientations are used to set the posture of an articulated body model. Details of the fabrication of a prototype MARG sensor are presented. Software implementation of the quaternion filter algorithms and a human body model designed to accept Earth-fixed reference orientation data are described. Calibration algorithms for the sensors and the human body model are also presented. Experimental results demonstrate the effectiveness of the tracking system and verify the correctness of the underlying theory.

14. SUBJECT TERMS Inertial Tracking, Magnetic Tracking, MARG Sensors, Complementary Filtering, Quaternions	15. NUMBER OF PAGES 27
---	---------------------------

		16. PRICE CODE
--	--	----------------

17. SECURITY CLASSIFICATION OF REPORT Unclassified	18. SECURITY CLASSIFICATION OF THIS PAGE Unclassified	19. SECURITY CLASSIFICATION OF ABSTRACT Unclassified	20. LIMITATION OF ABSTRACT UL
---	--	---	----------------------------------

NAVAL POSTGRADUATE SCHOOL
Monterey, California 93943-5000

RADM David R. Ellison, USN
Superintendent

Richard Elster
Provost

This report was prepared for NPS MoVES Academic Group
and funded by Army Research Office (ARO), Modeling and Simulation Office (N6M)

This report was prepared by:

Robert B. McGhee
Professor

Eric R. Bachmann
Research Assistant Professor

Xiaoping Yun
Professor

Michael J. Zyda
Professor

Reviewed by:

Released by:

Michael J. Zyda
Chair, MoVES Academic Group

D. W. Netzer
Associate Provost and
Dean of Research

Real-Time Tracking and Display of Human Limb Segment Motions Using Sourceless Sensors and a Quaternion-Based Filtering Algorithm - Part II: Implementation and Calibration

E.R. Bachmann, R.B. McGhee, X.P. Yun, and M.J. Zyda

Naval Postgraduate School, Monterey, CA
email: bachmann@cs.nps.navy.mil

Abstract

Rigid body orientation may be determined without the aid of a generated source using a nine-axis MARG (Magnetic field, Angular Rate, and Gravity) sensor containing three orthogonally mounted rate sensors, three orthogonal linear accelerometers and three orthogonal magnetometers. Part I of this paper described a quaternion-based complementary filter algorithm for processing the output data from such a sensor. This paper focuses on the implementation of that theory. It describes a system designed to determine the posture of an articulated body in real-time. In the system the orientation of each segment relative to an Earth-fixed reference frame is individually determined through the use of an attached MARG sensor. The orientations are used to set the posture of an articulated body model. Details of the fabrication of a prototype MARG sensor are presented. Software implementation of the quaternion filter algorithms and a human body model designed to accept Earth-fixed reference orientation data are described. Calibration algorithms for the sensors and the human body model are also presented. Experimental results demonstrate the effectiveness of the tracking system and verify the correctness of the underlying theory.

Introduction

Full body motion tracking is a necessity to the development of fully immersive virtual environments. Changes in body posture and position directly affect what is seen, heard, felt and smelled. The parameters sensed in the environment and the environment itself are altered and manipulated by the actions of the body. Thus, in order for a user to interact with a virtual environment in a natural way and have the virtual environment present appropriate information to the senses, it is imperative that data regarding body motion and posture be obtained.

Currently available motion tracking technologies are limited by their reliance on a generated signal or a necessity for the tracked body and fixed stations around a working volume to remain within sight of one another. In either case there is a requirement to maintain some type of link over a distance. The physical signal upon which the link is based may be generated electromagnetic fields, high frequency sound waves, light, or even radio waves. Regardless of the type of signal used, it can be generally referred to as a "source." Usually, the effective range over which the link may be maintained is limited. (Molet et al., 1999a) Update rates may be limited by the physical characteristics

of the source used. Interference with or distortion of the source will at best result in erroneous orientation and position measurements. (Nixon et al., 1998) If the link is broken, a complete loss of track will result. (Meyer et al, 1992; Durlach & Mayor, 1995) Significant gains in reliability and capability could be achieved through the development of a "sourceless" sensor technology that could determine orientation and position without using a link between fixed and mobile stations. Advances in the field of miniature sensors over the last decade make possible inertial/magnetic tracking of the three degrees of orientation of human body limb segments based on the passive measurement of physical quantities that are directly related to the rate of rotation and orientation of a rigid body. The "sourceless" nature of this technique makes possible full body posture tracking of multiple users over an area that is only limited by the range of a wireless LAN. Since orientation estimates are based only on passive measurements, nearly all latency in such a system is due to the computational demands of the data processing algorithms involved and not physical characteristics of the generated source.

The theory for a quaternion based complementary attitude estimation filter was developed in (McGhee et al., 2000a). The filter is designed to process data from a nine-axis MARG sensor containing three orthogonal angular rate sensors, three orthogonal linear accelerometers and three orthogonal magnetometers. Estimation error is minimized using Gauss-Newton iteration. Gains are constant, but may be tuned to fit a particular tracking situation. Due the use of quaternions to represent orientation, the filter is more efficient than similar Euler-angle based filters and avoids the singularities associated with Euler angle representation of orientation. Drift is corrected continuously without any requirement for still periods.

This paper presents a prototype inertial/magnetic human body tracking system. Individual limb segment orientations are estimated using MARG sensors and the algorithms developed in (McGhee et al., 2000a). The orientation estimates are used to animate a simple human model or avatar in real-time. The model directly accepts limb segment orientations relative to an Earth-fixed reference frame. The primary focus is on hardware and software implementation and the basic calibration procedures needed to make the system practical. These calibration procedures pertain to the MARG sensors themselves and the correction of offsets between the sensor frames and the frames associated with the limb segments to which they are attached.

Experimental results validate the theory in (McGhee et al., 2000a). Limited quantitative data document static stability, static convergence, and dynamic response and accuracy. Qualitative data video recordings allow conclusions to be reached regarding various modifications to the quaternion attitude filter algorithm and demonstrate the ability of inertial/magnetic body tracking to determine human-body posture in real-time.

Background

Though based upon well-established navigation algorithms, inertial and magnetic tracking is a relative newcomer to the human motion-tracking arena. It has been used to determine head orientation in virtual and augmented reality applications, but the development of a practical system for full body tracking applications has not yet been accomplished. Inertial sensing is finding expanded usefulness as a method of augmenting other motion tracking technologies.

A naive approach to inertial orientation tracking might simply involve only integration of angular rate data to determine orientation. However, this solution, which is found using only one type of sensor, would be prone to drift over time due to the buildup of small bias and drift errors. In order to avoid drift, inertial tracking systems make use of complementary sensors to continuously correct the orientation estimate. Commonly, these sensors include accelerometers to sense the vertical and a set of magnetometers to sense the direction of the local magnetic field. When combined, these two types can also be used to determine orientation. However, since the gravity vector cannot be found using linear accelerometers without averaging over some period of time, latency would be a problem in many applications. In order to track all orientations without significant latency, there must be a separate accelerometer, rate sensor and magnetometer for each of the three coordinate axes of a rigid-body.

Fuchs presented the first inertial/magnetic system for head tracking applications (Fuchs, 1993). This system utilized a fluid pendulum and three solid-state piezoelectric angular rate sensors. The initial system did not include a compass or magnetometers and thus drifted about the vertical axis. Subsequent systems include three orthogonal solid-state rate sensors, a two-axis fluid inclinometer and a two-axis fluxgate compass (Foxlin, 1996). InterSense, Inc. was started as a result of this research and continues to produce inertial tracking devices designed for head tracking applications. Most the systems currently marketed are hybrids that use ultrasonic range finding to determine or correct position. Sensor data is processed by a complementary separate-bias Kalman filter which requires periods of "still time" to correct for rate sensor drift. (Foxlin, 1996).

The fact that inertial data lends itself to prediction through the use of motion derivatives has resulted in the use of inertial sensors in numerous efforts to combat latency problems. In (Azuma, 1995), Azuma demonstrates that predicting future head location using three angular rate sensors and three linear accelerometers is an effective approach for significantly reducing dynamic errors in an augmented reality head tracking system. In this study, prediction caused the dynamic accuracy of HiBall head tracking system to increase by factors of 5 to 10. Linear Kalman filters are used to estimate and predict translation terms and an Extended Kalman Filter (EKF) is used to estimate and predict orientation terms.

(Foxlin, 1998) describes a hybrid outside-in inertial/acoustic system called the constellation. This system uses an inertial navigation system that is aided by ultrasonic time-of-flight range measurements. The inertial subsystem determines position through double integration of triaxial accelerometer data. The ultrasonic ranging system uses a "constellation" of ceiling mounted acoustic beacons in a manner very similar to the optical HiBall head tracking system. However, the ultrasonic system only calculates position. It does not calculate orientation. The stated reasons for using acoustic sensing as opposed to optical are cost, weight, and complexity. As with the HiBall system an extended Kalman filter is used to combine all sensor data and calculate an optimal position and orientation estimate. Acoustic range measurements are also individually processed using a SCAAT Kalman filter.

Inertial sensors such as those described in this research provide orientation relative to an earth fixed coordinate reference frame. In early inertial angle tracking work (Frey, 1996), Frey showed that an entire human body simulation could be built and animated using only orientation data for each body segment. This result eliminated the need for human

body motion capture systems to track the position of each body part and showed that orientation data alone could be used to determine body posture.

Usta created a human model designed to accept a quaternion representation of orientation relative to an earth fixed coordinate reference frame. The quaternions were then turned into rotation matrices for submission to the graphics API and the application of joint constraints (Usta, 1999). Qualitative results from his work are shown in Figure 1. Only static tests were performed. Other work has discarded the position data from active magnetic systems for posture determination and used only orientation data to drive the animation of a human model. This orientation data was used to determine joint angles that were applied to kinematic models (Skopowski, 1996; Molet et al., 1999b) Though Molet transmitted orientation quaternions across a network to save bandwidth, the quaternions were converted to rotation matrices. Inverse kinematic calculations were made to allow several joints to be driven with one sensor. Though a quaternion representation of orientation is used in the HiBall research described above, in each case the orientation is converted to an Euler angle representation. (Welch et al., 1999)

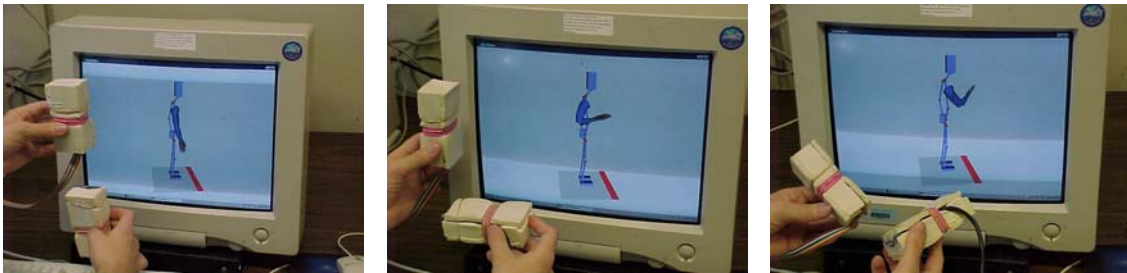


Figure 1: Inertial Motion Tracking of the Right Fore and Upper Arm with Two Inertia/Magnetic Sensors (Bachmann et al., 1999)

In orientation only tracking applications, position data for a single reference point is used only to place the entire human model within a virtual environment. Theoretically, it is possible to determine position as well as orientation using inertial sensors. This is done on a daily basis by the inertial navigation systems of submarines and other platforms, which must navigate without the aid of outside references. However, this dead reckoning performance is made possible through the use of very expensive and large sensors. Such dead reckoning is not possible with low-grade inertial sensors for anything longer than relatively short time periods (Bachmann et al., 1996; Foxlin, 1998). Without outside reference, position estimates based on low-quality sensors will drift in a manner similar to orientation estimates based only on angular rate sensors.

Prototype Inertial/Magnetic Body Tracking System

The prototype inertial/magnetic body tracking system in this research was implemented with several goals in mind. Among these goals were validation of the quaternion filter algorithm in a physical system, demonstration of the practicality and robustness of inertial and magnetic orientation tracking in real-time, and to provide a test-bed for further experiments. Several features are considered imperative if these goals are to be met. Among these are:

- Orientation tracking of any three or more human limb segments using nine-axis MARG sensors
- Sufficient dynamic response and update rate (100 HZ or better) to capture fast human body motions
- Ability to change quaternion filter operating parameters while the system is in operation
- Calibration of individual sensors without the use of any specialized equipment
- Simplified human kinematic model based entirely on quaternions capable of accepting orientation parameters relative to an earth fixed reference frame in quaternion form
- Automatic accounting for the peculiarities related to the mounting of a sensor on an associated limb segment

System Hardware

Figure 2 is a diagram of the prototype system hardware. Depicted are three body-mounted MARG sensors outputting analog signals to three I/O connection boards. The output from each connection board is digitized by an associated A/D converter card. The cards themselves are mounted in a standard Wintel desktop computer. All data processing and rendering calculations are performed by software running on this single processor machine.

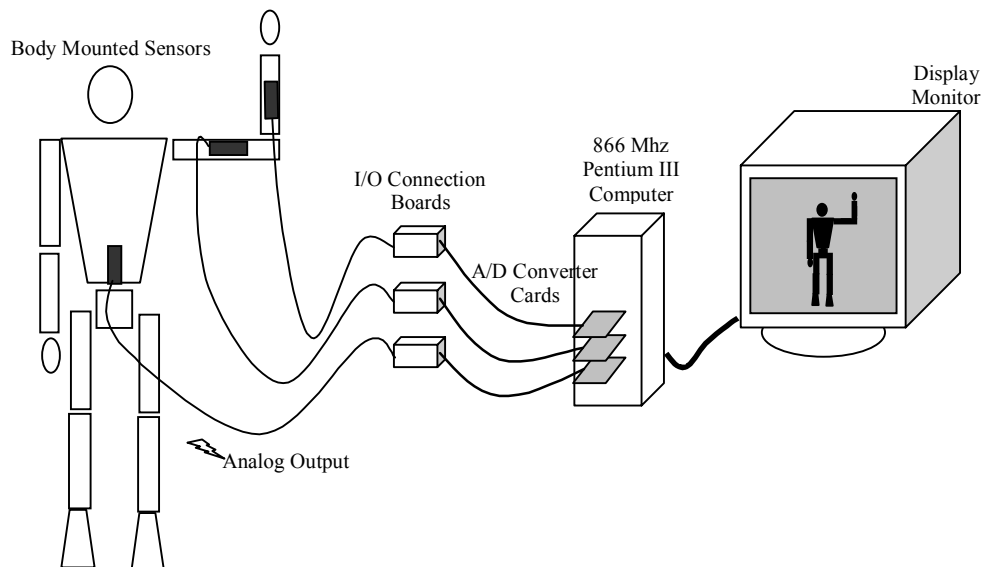


Figure 2: Prototype Inertial and Magnetic Body Tracking System (Bachmann, 2000)

MARG Sensors

To track the entire human body, approximately fifteen nine-axis units would be required. One sensor would be attached to each limb segment to be tracked. The exact number of sensors needed would depend upon the desired motion tracking detail to be captured. Three such sensors were used in the system described here.

The prototype MARG sensors used in this research (Figure 3) were custom built using off-the-shelf, low cost components. Each sensor package measures 10.1 x 5.5 x 2.5

cm. The analog output of the sensor is connected to a breakout header via a thin VGA monitor cable. Output range is 0-5 vdc. The power requirement of the sensors is 12 vdc at approximately 50 milliamperes. The primary sensing components are a Crossbow CXL04M3 triaxial accelerometer (Crossbow, 1998), a Honeywell HMC2003 3-axis magnetometer (Honeywell, 1998) and three Tokin CG-16D series miniature angular rate sensors mounted in an orthogonal configuration (Tokin, 1998). The individual components are integrated using a single integrated circuit board with the accelerometers mounted separately. The circuit provides a set/reset circuit capability for the magnetometers and allows manual adjustment of magnetometer null points. Rate sensor output voltage is amplified by a factor of five and filtered to attenuate rate sensor oscillator noise. All three MARG sensors were fabricated by McKinney Technology of Prunedale, California (McKinney, 2000).

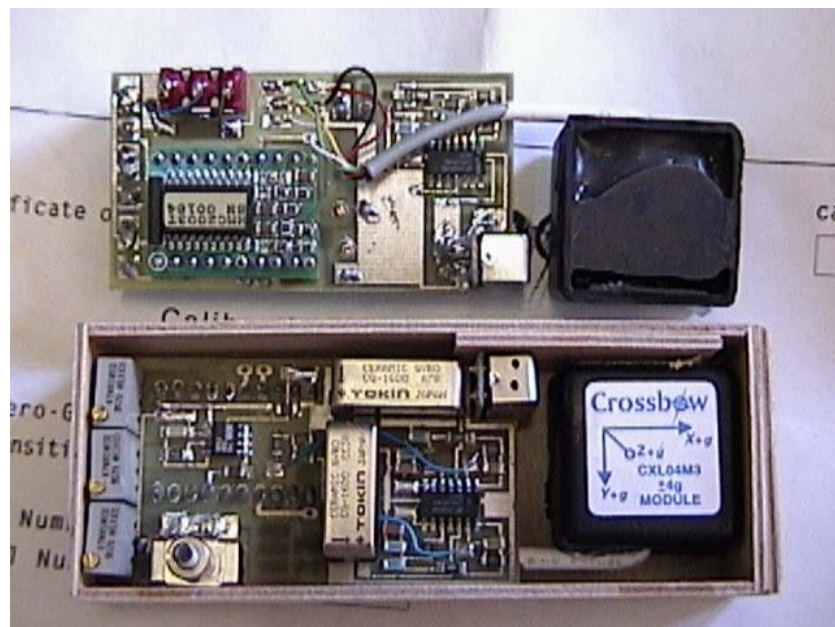


Figure 3: Prototype MARG Sensor (McKinney, 2000)

Rate Sensor Bias Compensation

In earlier body tracking work, the angular rate sensors were bias compensated in software (Bachmann et al., 1999). In the research described in this document, the hardware is considered stable enough to eliminate the need for these additional calculations. However, integration of a biased angular rate signal will cause a steady state error in a complementary filter. In order to achieve better system performance, this correction should be hardware implemented in the rate sensor conditioning circuitry using capacitive coupling. Such a bias compensation circuit is depicted in Figure 3.

RATE SENSOR SIGNAL CONDITIONING

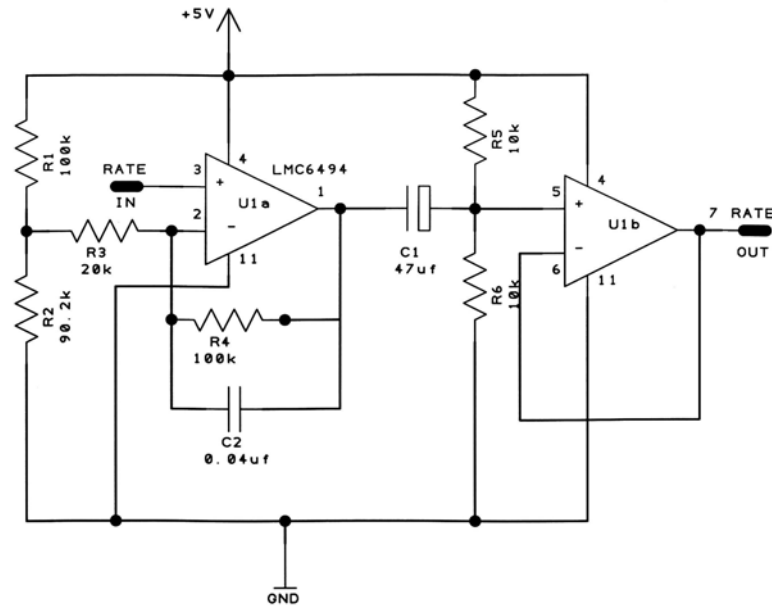


Figure 3: MARG Rate Sensor Bias Compensation Circuit Schematic (McKinney, 2000)

Magnetometer Set/Reset

Early system testing was hampered due to saturation of the MARG sensor magnetometers by small magnetic fields. Saturation produced flips or reversals resulting in changes in the sensor characteristics. Once saturated, the lack of a built-in reset made it difficult to restore the magnetic sensors to a usable condition. Only through repeated exposure to various magnetic fields and trail and error iterations could the sensors be returned to a functional condition. Often, the magnetometer null points had changed following these procedures making it necessary to recalibrate the sensor.

Manufacturer's literature states that HMC1001/2 magnetometer saturation occurs due to the influence of a strong magnetic field in excess of 30 gauss, which can cause the polarity of the MR film magnetization to flip (Caruso, 1995). In practice, changes in the magnetometer characteristics were found to occur in the presence of weaker fields such as those caused by exposure to metal scissors or cell-phones. Following such an upset field, a strong restoring magnetic field must be momentarily applied to restore, or set, the sensor characteristics. The effect is commonly referred to as applying a set or reset pulse. The Honeywell HMC1001/2 incorporates a patented on-chip strap for performing the re-magnetization electrically. This flipping may be performed manually or automatically at various time intervals. (Caruso, 1995)

The sensors used in this research incorporate a manual set/reset circuit to electrically restore the magnetometers to proper operation. Activation of the circuit is accomplished using a sensor-mounted button. The associated circuit is depicted in Figure 4. The purpose of the circuit is to set or reset the permalloy film contained in the

individual magnetometers by applying a current pulse of 3-4 amps for approximately 20-50 nsec.

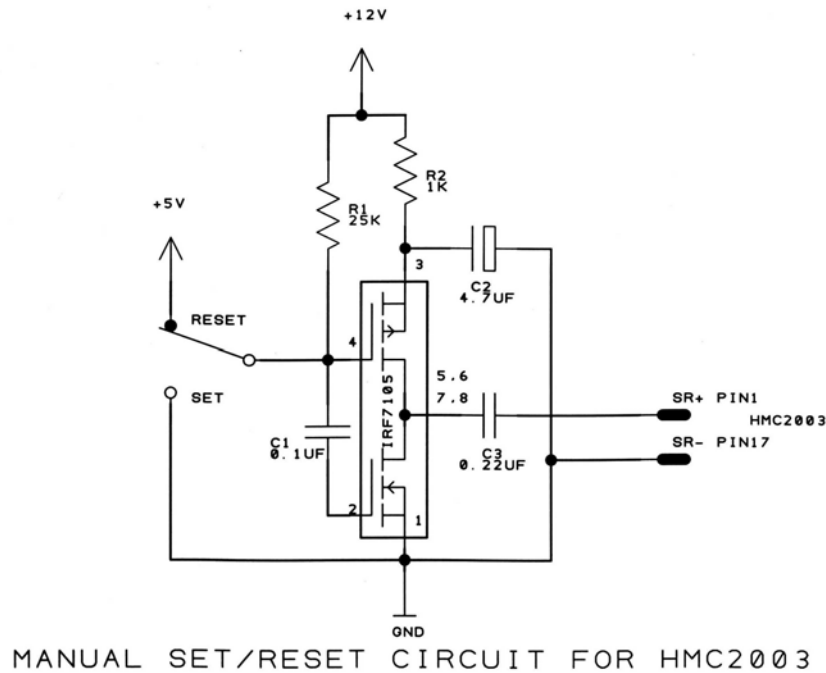


Figure 4: MARG Sensor Magnetometer Set/Reset Circuit Schematic (McKinney, 2000)

Incorporation of an analog to digital converter (ADC) directly into the MARG sensor would ease data handling. The ADC could also automate the magnetometer set/reset circuit by providing clocked and, therefore, constant readings of set and reset produced magnetic data. Using the difference of the two magnetic readings taken during the set/reset cycle will result in magnetic data that is automatically temperature compensated.

System Software

The system software implements the estimation as well as calibration algorithms which make possible tracking of human body segments using MARG sensors. Drift correction is performed using the reduced order form of Gauss-Newton iteration described in (McGhee et al., 2000). Facilities are included to allow performance of experiments related to differential weighting of magnetometer and accelerometer data, variation of intervals between drift corrections, and adjustment of the filter gains.

A sensor calibration algorithm allows system users to calibrate individual sensors by subjecting them to a series of six 90 or 180 degree rotations followed by two 360-degree rotations oriented with respect to the local magnetic field.

In addition, the system software includes a fully articulated human model based entirely on quaternion/vector pairs (Funda, 1990). No rotation matrices are used to position the model. Limb segments are oriented independently of one another and positioned through the addition of limb associated vectors. The model is positioned and oriented relative to a z-axis down coordinate system (McGhee et al., 2000b).

The software for this research is fully object oriented. It was written in C++. Estimation and rendering events are window system timer driven at 100 Hz and 25 Hz respectively. The code is single threaded. It runs on a standard 866 MHz Intel Pentium III platform under the Windows 2000 operating system.

Sensor Calibration

In order for the system to operate properly, it is imperative that the null point and scale factor of each individual component of the MARG sensors be determined prior to commencing limb tracking. The null point and scale factor for each component are found through the following calibration procedure. Unless the characteristics of the sensors themselves change, calibration need only be accomplished once. However, due to variations in the direction of the local magnetic field vector, better performance is to be expected if the direction of this reference is determined before each tracking session.

An individual linear accelerometer can be calibrated by placing it in a vertical position to sense gravity in one direction and then turning it over to sense gravity in the other. Half way between the readings taken is the null point.

$$accel\ null = \frac{accel\ max + accel\ min}{2} \quad (1)$$

Multiplication of a correct scale factor times the accelerometer output values will result in a product of 1 g in one direction and -1 g in the other. This scale factor can be found using

$$accel\ scale = \frac{(accel\ units) \times 2}{accel\ max - accel\ min} \quad (2)$$

Calibration of a triaxial accelerometer module is accomplished in a similar manner. The MARG unit is placed in six different positions so that each individual accelerometer can sense gravity along both its negative and positive axes.

An obvious method of magnetometer calibration is very similar to that used for accelerometers. Instead of orienting each sensor relative to the gravity vector, each magnetometer would have to be placed in a position in which it can sense the maximum strength of the local magnetic field along both its negative and positive axes. This can be accomplished by pointing the magnetometer axis towards the local magnetic north and recording the maximum and minimum voltages as the magnetometer is rotated 360 degrees about an axis oriented toward the east. Half way between the maximum and minimum readings obtained is the null point of the magnetometer.

$$mag\ null = \frac{mag\ max + mag\ min}{2} \quad (3)$$

Multiplication of a correct scale factor times the magnetometer output values should result in a reading of approximately 0.6 gauss in one direction and -0.6 gauss in the other depending upon the actual strength of the local magnetic field.

$$mag\ scale = \frac{(mag\ units) \times 2}{mag\ max - mag\ min} \quad (4)$$

Complete calibration of a three-axis magnetometer could thus be accomplished by performing one such rotation for each individual sensor.

Determination of the null point of an angular rate sensor can be accomplished by recording and averaging over some time period the output of a static sensor. Scale factors

are determined by integrating the output of angular rate sensor over time. If an angular rate sensor is subjected to a known angle of rotation and its output is integrated during the period of rotation, the correct scale factor will cause the result of that integration to equal the angle of rotation. The scale factor for a rate sensor can therefore be determined following a known rotation using

$$scale\ factor = \frac{known\ rotation}{estimated\ rotation} \quad (5)$$

where the estimated rotation term is the result of integrating the output of the sensor with a scale factor of unity. In practical applications it may be desirable to make several estimates of the scale factor while putting the sensor through several known positive and negative rotations and then averaging the results.

From the above, it is apparent that a MARG sensor can be completely calibrated using a level platform and a simple compass to indicate the direction of the local magnetic field. In this research each sensor was calibrated by placing it in six positions which allowed each accelerometer to sense gravitation acceleration in both the positive and negative directions, subjecting each rate sensor to one or more known rotations and rotating the MARG sensor in a manner such that maximum and minimum local magnetic field readings can be obtained for each magnetometer.

Once the magnetometers have been properly calibrated, the MARG sensor is used to determine the direction of local magnetic field vector. This is accomplished by placing the sensor in a reference position on a level non-metallic surface with the x-axis of the sensor aligned with the local magnetic north. The readings received from the three orthogonal magnetometers while the sensor is in this position correspond to the three components of the vector desired.

The steps of the sensor calibration algorithm listed in Appendix B loosely correspond to the actual physical actions that a person doing the calibration must perform upon the sensor. The entire calibration procedure is directed by the software and can be performed in less than one minute. Multiple sensors could be calibrated simultaneously by placing the sensors in a “box” containing a bin for each sensor. The box itself would be subjected to the same sequence of rotations and orientations as those described above for an individual sensor

Quaternion Attitude Filter

The *CQuatAttFilter* class implements the reduced order quaternion attitude filter described in (McGhee et al., 2000). With the exception of the measured rate quaternion, \dot{q} , (Eq. (26)) and the correction quaternion, \dot{q}_e (Eq. (25)), all quaternions are normalized to unit length. The reference unit vectors, m and n , used in Eq. (13) and Eq. (14) respectively are determined during the calibration process. Expected input to the class objects is nine floating-point numbers corresponding to the nine analog output voltages of an associated MARG sensor. These are used to construct the measured gravity vector (h in Eq. (15)), the measured magnetic field vector (b in Eq. (16)) and the body rate vector (${}^B\omega$ in Eq. (26)).

Once a *CQuatAttFilter* object has been instantiated and estimation has begun, the *estimateRotation* method serves as the primary interface to obtain updated orientation estimates. The returned quaternion object represents the estimated orientation of the

associated MARG sensor block relative to an Earth-fixed reference frame. Figure 5 depicts the control logic flow and the step-by-step algorithm followed by this method. Appendix A provides a step-by-step explanation of the mathematical calculations performed during each of the superscripted steps in the figure.

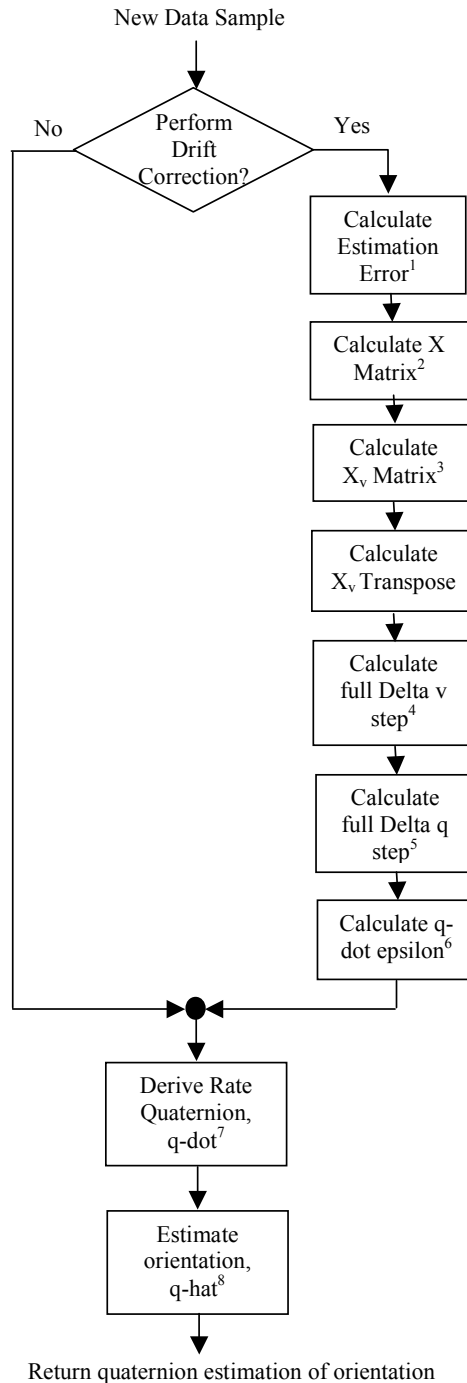


Figure 5: Orientation Estimation Flow Chart (Bachmann, 2000)

Quaternion Based Human Body Model

The vertices of an individual segment of the human model are described relative to a z-axis down coordinate system that is attached to the inboard end of the segment. If the sensor and limb segment coordinate axes are aligned, the orientation of an individual limb segment could be set by applying to each vertex, v , the quaternion rotation

$$q_{sensor} \otimes v \otimes q_{sensor}^* \quad (6)$$

where the unit quaternion q_{sensor} is the estimated orientation produced by the filter processing the sensor output data and q_{sensor}^* is its conjugate.

Due to the irregular shape of human limb segments and other factors related to sensor mounting and attachment, it is difficult to achieve perfect alignment between the sensor and limb segment axes. This misalignment can be taken into account by performing an additional fixed rotation using an offset quaternion

$$q_{sensor} \otimes q_{offset} \otimes v \otimes q_{offset}^* \otimes q_{sensor}^* \quad (7)$$

to each vertex, where q_{offset} is the offset quaternion for the limb of the vertex.

When the human model is in the reference position, the limb segment coordinate axes are aligned with the corresponding Earth-fixed axes. That is the x-axis for each limb segment points toward the local north, the y-axis points east and the z-axis points down. The offset quaternion for each limb segment can be derived by noting that while the user is in the reference position the equation

$$v = q_{sensor} \otimes q_{offset} \otimes v \otimes q_{offset}^* \otimes q_{sensor}^* \quad (8)$$

holds true. This implies that

$$q_{sensor} \otimes q_{offset} = 1 \quad (9)$$

This result and the inverse law of quaternion multiplication further implies that the offset quaternion can be found while in the reference position using

$$q_{offset} = q_{sensor}^{-1} = q_{sensor}^* \quad (10)$$

Complete compensation for the way in which all sensors are attached to the limbs of a tracked subject can therefore be accomplished by simply setting q_{offset} for each limb segment to the inverse of the associated q_{sensor} while the subject to be tracked is standing in a predetermined reference position. The implemented reference position for this research is an ‘‘attention’’ stance facing the local magnetic north. The calculated offset quaternion will remain valid as long as the sensor positions do not shift position relative to the tracked limb segment.

To set the position of an individual limb segment it is necessary to find a vector that describes the location of the inboard end of the limb segment. Once this vector is found the final position of each vertex can be calculated through addition of this vector to the rotated coordinates of each vertex. Thus, the final position of a limb segment vertex is given by

$$p_{trans} + q_{sensor} \otimes q_{offset} \otimes v \otimes q_{offset}^* \otimes q_{sensor}^* \quad (11)$$

where p_{trans} is a vector describing the location of inboard end of the limb.

Each limb segment has an associated translation vector, p , which extends from the inboard to the outboard end of the segment. Once this vector has been oriented using Eq. (7) the outboard end point can be used as the origin location for the coordinate system of more distal segments attached to the end point. Thus, p_{trans} in Eq. (8) is simply the vector

sum of rotated translation vectors associated with limb segments that are between the body origin and the limb segment being positioned.

System Performance

Quantitative and qualitative results document the accuracy and robustness of the system under various dynamic and static conditions. The static experiments described relate to the stability, convergence properties, and accuracy of the orientation estimates produced by the quaternion attitude filter algorithm when processing MARG sensor data. The qualitative experiments examine the performance of the system as a whole in relationship to the goal of robust posture estimation. The performance of the system while using differential weighting of sensor data as well as increased drift correction intervals is investigated. The ability of the system to track the posture of various limb segments of the human body using three MARG sensors is also evaluated.

Static Stability

The drift characteristics of the quaternion filter algorithm and the MARG sensor over extended periods were evaluated using static tests. In each of these experiments the stability of the orientation estimate produced with the sensor stationary was monitored for a specified period.

Figure 6 graphically depicts the drift of each of the four components of the quaternion estimate produced by the filter over a one-hour period. It can be observed that average total drift is about 5%. During the experiment shown, the filter gain, k (Eq. (25)), was set to unity. Equal weighting was given to both magnetometer and accelerometer data. It is expected that increasing the filter gain to 4.0 would reduce the drift error by a factor of four. However, due to the observed stability of the filter over a one hour period, no further static experiments relating to stability were conducted. Other experiments also indicated that nearly all instability observed was due to a design error in the MARG sensor angular rate-bias compensation circuitry. That is, at the time of the test the capacitor coupling of Figure 3 had not yet been installed. It is anticipated that this change will remove almost all of the effects of rate sensor drift. Such a modification is now in progress and will be used in further system testing.

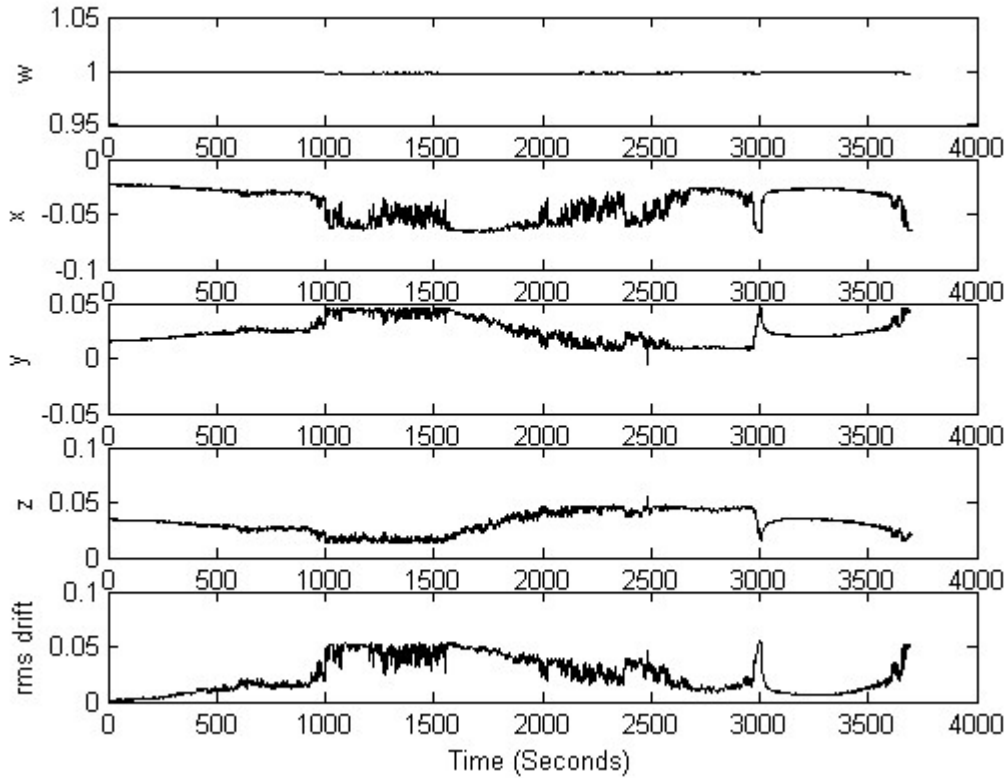


Figure 6: One Hour Static Test of Orientation Estimate Stability, $k = 1.0$ (Bachmann, 2000)

Static Convergence

Linear analysis of the quaternion filter and nonlinear simulation imply the transient errors will persist for a time period that is inversely proportional to the filter gain. Specifically, by the time

$$t = \frac{1}{2k} \quad (12)$$

following the occurrence of a transient error, it is expected that the magnitude of the square of the error should be reduced to 37%. (Bachmann, 2000)

Experiments to test the static convergence of the filter following transient errors were conducted to further validate the results of the linear analysis. The MARG sensor itself was left in a stationary position throughout each of these experiments. Transient orientation errors were introduced into the system by rotating a stable estimate by an error quaternion. Following this rotation, the filter was allowed to re-converge to the previous estimate. Error quaternions representing orientation errors of 30 degrees were used. Filter gains included 1.0, 4.0, 8.0, 16.0 and 32.0. In each of these experimental trials the filter remained stable and re-converged to the previous estimate in the time period predicted by linear theory. Figure 7 plots the magnitude of the quaternion filter criterion function (Eq. (19)) versus time.

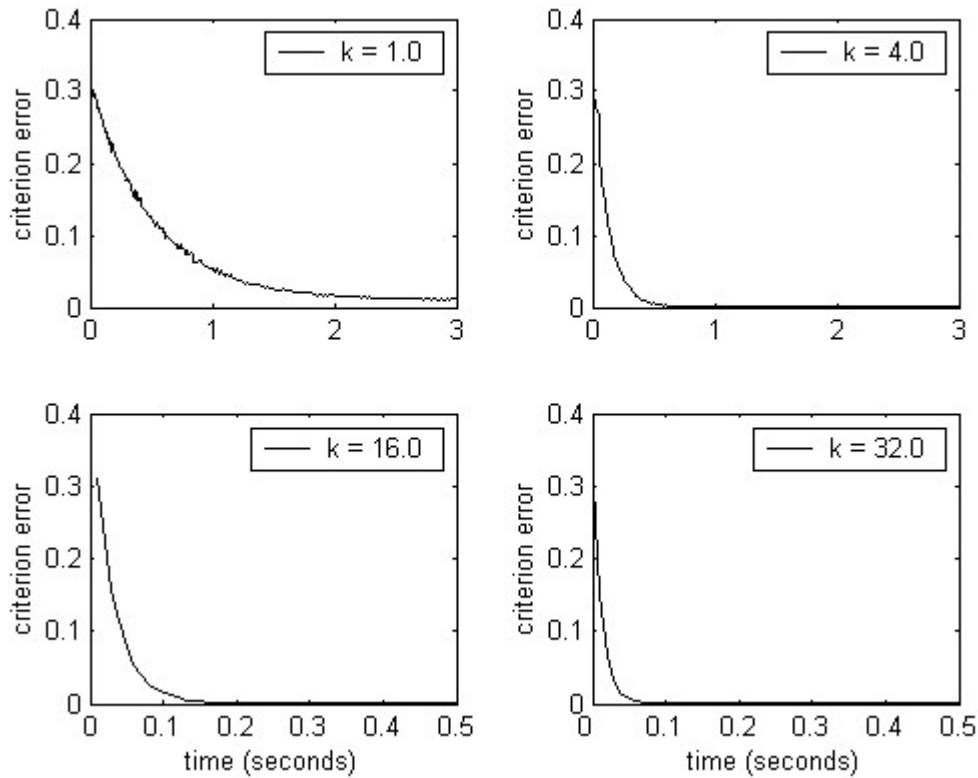


Figure 7: Error Convergence Following 30 Degree Transient Errors (Bachmann, 2000)

Dynamic Response and Accuracy

Preliminary experiments were conducted to establish the accuracy of the orientation estimates and the dynamic response of the system (Bachmann et al., 1999). These experiments were completed using a Hass rotary tilt table (Haas, 1992). The preliminary test procedure consisted of repeatedly cycling the sensor through various angles of roll, pitch and yaw at rates ranging from 10 to 30 deg./sec. After each motion, the table was left static for approximately 15 seconds. The estimates produced by the tracking system were converted to Euler angle form for easier comparison to the tilt table rotations. Figure 8 is a typical result of the dynamic accuracy experiments. In the depicted experiment, the sensor was rotated back and forth from 0 to 45 degrees at a rate of 10 degrees per second. It is observed that the tracking accuracy of the sensor is within one degree.

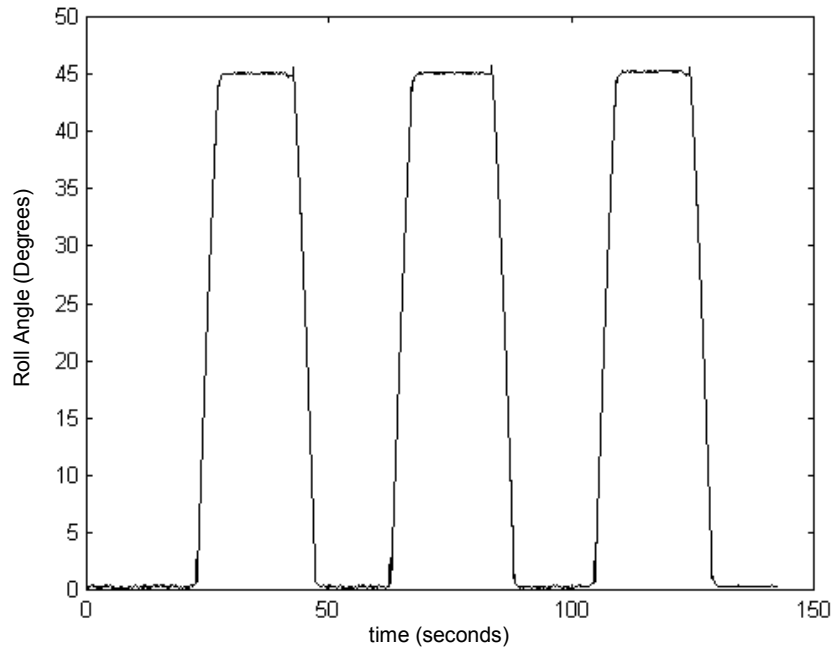


Figure 8: 45 Degree Roll Excursions at 10 Degrees/Second (Bachmann et al., 1999)

Weighted Least Squares

Significantly reducing the weight given to magnetometer data will allow drift about the vertical axis. However, limited reductions may also make it possible to avoid large transient rotations about the vertical axis in the presence of changing magnetic fields. The weighted least squares modification to the quaternion filter algorithm is designed to allow orientation estimation to continue in the presence of changing magnetic fields. (McGhee et al., 2000)

To examine the weighted least square function of the filter, a MARG sensor was repeatedly subjected to a magnetic source. In each trial a speaker magnet was passed over the sensor at a distance of approximately 1 cm. Magnetometer weighting values, ρ , of 0.25, 0.5, and 1.0 were used. The filter gain, k , was 4.0 in all trials. Figure 9 plots the rms difference between the orientation estimate before and following exposure to the magnet induced field. As expected, using a lower magnetometer weighting factors allow a greater immunity to magnetic field disturbances.

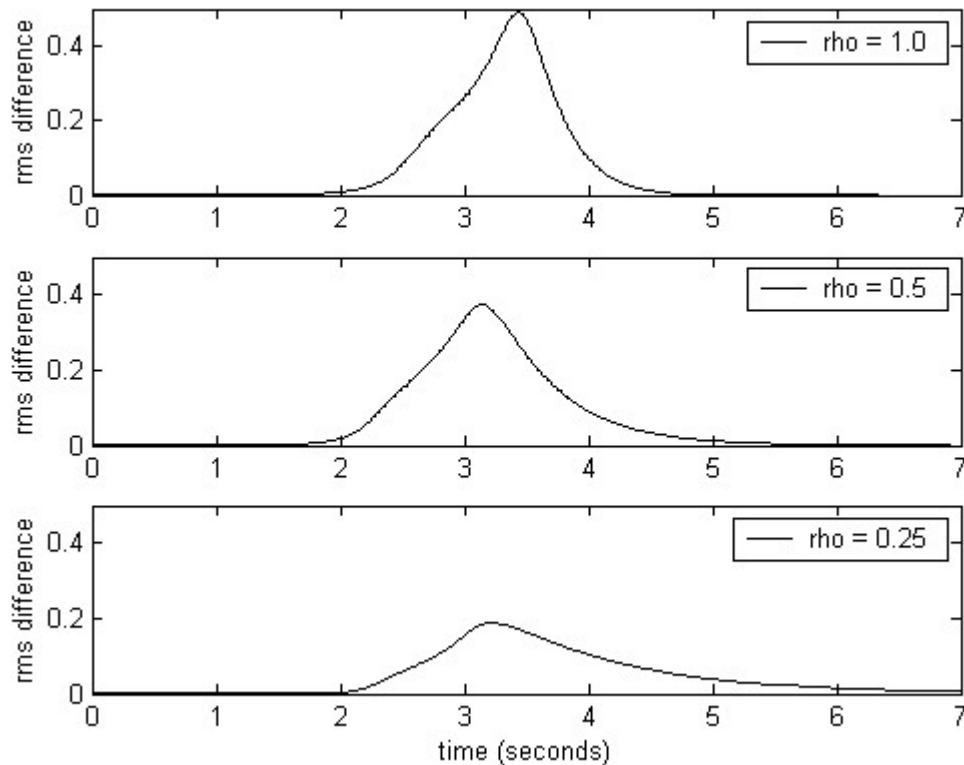


Figure 9: rms Change in Orientation Estimate During Exposure to Magnetic Field (Bachmann, 2000)

Posture Estimation

The purpose of the human body tracking system is to estimate the orientation of multiple human limb segments and use the resulting estimates to set the posture of the human body model that is visually displayed. Numerous experiments were conducted to qualitatively evaluate and demonstrate this capability. In each experiment three MARG sensors were attached to the limb segments to be tracked. Due to the minimal number of sensors available tracking was limited to a single arm or leg. In the case of arm and limb segments, sensor attachment was achieved through the use of elastic bandages. In most cases this method appeared to keep the sensors fixed relative to the limb. Body tracking was performed using various gains. Video recordings of the system in normal operation indicate that posture estimation was accurate and showed very little lag. Figure 10 depicts inertial tracking of various limb segments. A quicktime movie of these experiments may be downloaded at <http://npsnet.org/~bachmann/research.htm>

Accelerometer/Magnetometer Only Tracking

Experiments conducted with no rate sensor data input showed that the system could accurately determine posture in applications not involving rapid movement using only accelerometers and magnetometers. To attempt the capture of fast motions the filter gain was increased to higher values. This made the system more responsive, but also resulted in overshoots following the completion of a quick motion. These overshoots are most likely the result of the inability of the filter to accurately distinguish between

gravitational and linear acceleration when using the higher gain values. Overall, the performance of the system without rate sensors indicates that a less expensive system could be constructed using six axis sensors containing only accelerometers and magnetometers. Such a system would function well in low acceleration applications. It would not however be appropriate to feedback control applications requiring a quicker response. (McGhee et al., 1986)

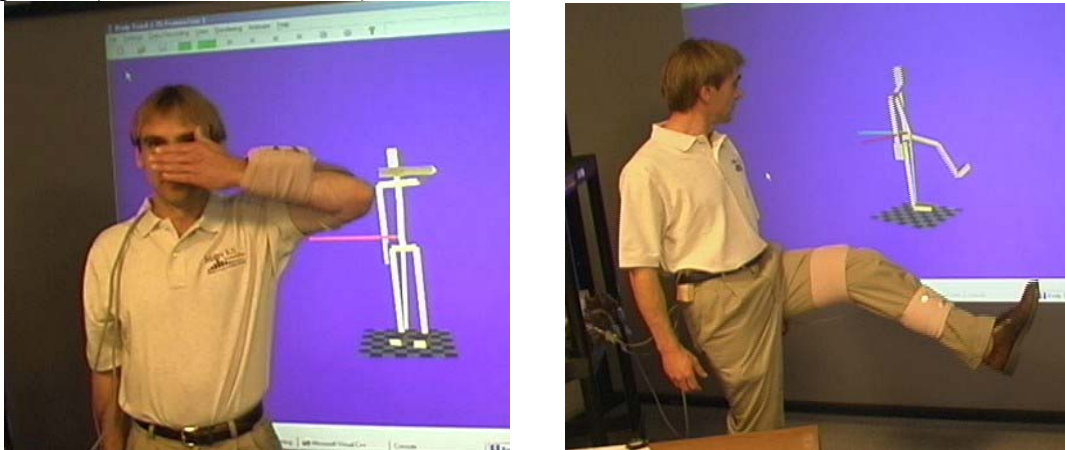


Figure 10: Inertial/Magnetic Tracking of Arm and Leg Using Three MARG Sensors (Bachmann, 2000)

Reduce Rate Drift Correction

In viewing Figure 5, it is apparent that the computational expense of calculating drift corrections based upon magnetometer and accelerometer data is much higher than merely updating the orientation estimate using only rate sensor data. Derivation of the X matrix in the “Calculate X Matrix” step requires the computation of multiple partial derivatives and inversion of a 3×3 matrix.

If the drift time constant of the rate sensors is long enough and the noise level is low, a drift correction is not be required on every filter cycle. Eliminating the need to perform drift correction calculations on every filter cycle leads to a significant reduction in computational costs of running the filter. This reduction may be taken advantage of in two different ways. Reducing the number of drift corrections can be used to increase the overall update rate of individual filters or increase the number of filters which may be operated with given amount of processing power.

To test this hypothesis, posture estimation was evaluated qualitatively while operating three actual and 13 simulated filter software objects. Filter update rates were maintained at 100 Hz. However, only one filter object performed drift correction calculations on each update cycle. This was equivalent to performing drift correction computations for each filter object at a rate of approximately 6 Hz. Filter gains were not changed to compensate for this modification since the most recently derived drift correction factor was still used on every update cycle. Qualitative evaluation of posture tracking indicated the effects of increasing the drift correction interval for each filter object were negligible.

InterSense InertiaCube Comparison

Qualitative evaluation of an InterSense IS-300 orientation tracking system was completed using both the manufacturers demonstration software and the body tracking software

developed for this research. When using the demonstration software the basis of the InterSense filter in Euler angles becomes apparent each time the *InertiaCube* sensor is subjected to a pitch angle approaching +/- 90 degrees. In this attitude the roll and yaw values gyrate widely while maintaining a constant sum or difference. When tested with the body tracking software implemented as part of this research, the system was configured to output a quaternion representation of orientation. While operating in this mode it was not possible to detect any singularities due to the internal use of Euler angles to represent orientation.

InertiaCube data is processed by a complementary separate-bias Kalman filter which requires periods of "still time" to correct for rate sensor drift. (Foxlin, 1996). While the inability to continuously correct for drift may not be a drawback in many head tracking applications, it is hypothesized that the filter may not function properly in constant high acceleration applications such as full body tracking. The ability of the InertiaCube to correct for rate sensor drift was tested by subjecting the sensor to a series of accelerations and then placing it on a flat surface. When using either the demonstration application or the body tracking software, the system exhibited its inability to correct for drift unless in a stationary state. Each time the sensor was replaced on the flat surface the orientation estimate failed to match the true orientation for a short time period before making a correction. This phenomenon occurred regardless of the operating mode of the InterSense system and is in marked contrast to continuously corrected estimates produced by the MARG sensor and the quaternion attitude filter algorithm. Again, a video record of these experiments is available at <http://npsnet.org/~bachmann/research.htm>

Future Work

Current technology will permit the construction of sensors that are much smaller than the prototype MARG sensors described here. An optimal inertial sensor would have the same size and form factor as a wristwatch. It would include an embedded microprocessor on which the filter algorithm is implemented as well as an analog to digital converter. The sensor would have a self-contained power source and would wirelessly transmit orientation data. Efforts are currently being made to untether the user of the sensor system by feeding MARG sensor data to a wearable computer. The wearable PC digitizes sensor data and transmits them to a fixed workstation via an 802.11b wireless LAN. Bluetooth technology (Bray & Sturman, 2000) is being investigated as a means to create a completely wireless sensor. Use of Bluetooth will enable sensors to wirelessly transmit data from body extremities to the wearable PC.

In order to ensure that the user can effectively interact with the virtual environment, the model used by the inertial tracking system must be scaled to the user's dimensions (Skopowski, 1996). This type of calibration ensures that, for example when a subject touches their right shoulder with their left fingertips, their avatar representation will do so as well. Organizations such as US Marine Corps routinely perform laser scans to obtain very accurate data on the exact size of an individual. Work is currently underway to develop methods for creating efficient models based on such data that can be driven by world-reference frame orientation data. These models would be perfectly sized for each individual. (Dutton, 2001)

Filter research has continued with the development of an extended Kalman Filter for real-time estimation of rigid body orientation (Marins, 2000). Non-real-time static and dynamic testing of the filter has been performed with synthetic data and real sensor data. Kalman filtering is highly dependent on the quality of the incorporated process model. When applied to human body motion tracking, Kalman filter design requires an adequate dynamic model of the human musculoskeletal system, and the measurement statistics of the MARG sensors (Brown & Hwang, 1992). Dynamic models of the musculoskeletal system are well established and widely used for computer simulations of human body motions (Harris & Smith, 1996; Koozekanani et al., 1983). These models are given in the form of second order differential equations containing parameters representing body segment mass, center of mass, and moments of inertia. Though these models are ideal for computer simulations of human body motions, they are computationally too complex to work in a system requiring real-time tracking of multiple users wearing multiple sensors. One possible approach to the modeling problem might be to develop a model in which each limb segment is considered independently of the others. This approach suggests that the process model needed for Kalman filtering may not need to make use of articulated body models, but could treat each limb segment as a single rigid body moving under the influence of forces produced by muscles and connective tissues (Yun et al., 1999; Frey, 1996) The availability of reliable MARG sensors allows the gathering of statistical data needed to construct such a model.

The ultimate goal of this project is to insert humans into a networked virtual environment. A network of 15 MARG sensors will track body posture. In order to accurately place the icon of the user in the virtual environment, it will be necessary to know body location as well as the posture of the body. To achieve this, the position of one body limb segment must be tracked. Radio Frequency (RF) positioning systems are very fast and long range by their nature. Large working volumes can be covered using a minimal amount of equipment and positional error magnitudes remain constant throughout. RF positioning systems can penetrate objects, walls, and the human body, and are able to operate with no line-of-sight. Although several technical challenges exist (IntegriNautics, 2000), RF positioning is still seen as the technology which will best complement the sourceless capabilities of inertial/ magnetic sensing and enable tracking of a multiple users over a wide area. While indoor tracking of this type is still under development, currently available differential GPS may provide adequate position tracking for some outdoor applications.

Summary and Conclusions

This research has demonstrated an alternative technology for tracking the posture of an articulated rigid body. The implemented system tracks human limb segments accurately with a 100 Hz update rate. The technology is based on the use of inertial/magnetic sensors to independently determine the orientation of each link in the rigid body.

At the core of the system is an efficient complementary filter that uses a quaternion representation of orientation. The filter can continuously track the orientation of human body limb segments through all attitudes without singularities. Drift corrections are made continuously with no requirement for still periods. Though the filter is nonlinear, physical experiments demonstrate that linear analysis of the filter is relevant and can be used as a method for selecting scale factors and predicting performance.

The filter processes data from MARG sensors, which contain components typically combined to form an inertial navigation system. Methods for conditioning and digitizing the output of the individual components are presented. Sensor calibration is achieved using a novel calibration routine, which requires no specialized equipment.

Articulated body posture is represented using a model based entirely on quaternion/vector pairs. Individual limb segments are oriented independently using a quaternion representation of the orientation relative to an earth-fixed reference frame. The underlying simplicity of the model makes possible a quick and accurate calibration calculation that compensates for misalignments between sensor and limb segment coordinate axes.

Due to its sourceless nature, inertial/magnetic tracking could overcome many of the limitations of motion tracking technologies currently in wide spread use. Combined with an appropriate positioning system, it is potentially capable of providing wide area tracking of multiple users for synthetic environments and augmented reality applications.

Acknowledgements

The authors wish to acknowledge the support of the U. S. Army Research Office (ARO) under Proposal No. 40410-MA and the U. S. Navy Modeling and Simulation Management Office (N6M) for making this work possible.

References

Azuma, R. (1995) *Predictive Tracking for Augmented Reality*, Ph.D. Dissertation, University of North Carolina at Chapel Hill, Computer Science Technical Report TR#95-007, Chapel Hill, NC.

Bachmann, E., Duman I., Usta, U., McGhee R., Yun, X., & Zyda, M. (1999). "Orientation tracking for Humans and Robots Using Inertial Sensors," *International Symposium on Computational Intelligence in Robotics & Automation (CIRA 99)*, Monterey, CA, pp.187-194.

Bachmann, E. (2000). Inertial and Magnetic Angle Tracking of Limb Segments for Inserting Humans into Synthetic Environments, Ph.D. dissertation, Naval Postgraduate School, Monterey, CA. (Available at <http://npsnet.org/~bachmann/>)

Bachmann, E., McGhee, R., Whalen, R., Steven, R., Walker, R., Clynch, J., Healey, A., & Yun, X. (1996). "Evaluation of an Integrated GPS/INS System for Shallow-water AUV Navigation (SANS)," *Proceedings of the IEEE Symposium on Autonomous Underwater Vehicle Technology, AUV '96*, Monterey, CA, pp. 268- 275.

Bray, J. & Sturman, C. (2000). *Bluetooth: Connect without Cables*, Prentice Hall, Inc.

Brown, R. & Hwang, P. (1992). *Introduction to Random Signals and Applied Kalman Filtering, Second Edition*, John Wiley and Sons, Inc., New York, NY.

Caruso, M. (1995). *Set/Reset Pulse Circuits for Magnetic Sensors*, Honeywell, Inc., AN-201.

- Crossbow Inc., (1998). *Crossbow CXL04M3 Data Sheet*.
- Durlach, N. & Mayor, A. (Eds.) (1995). *National Research Council, Virtual Reality: Scientific and Technological Challenges*, National Academy Press, Washington, D.C., pp. 188-204, 306-317.
- Dutton, A. (2001). *A Realistic Articulated Human Avatar from Laser Scan Data*, Master's Thesis, Naval Postgraduate School, Monterey, CA.
- Foxlin, E. (1998). "Constellation: A Wide-Range Wireless Motion-Tracking System for Augmented Reality and Virtual Set Applications," *Proceedings of SIGGRAPH '98*, ACM, pp. 371-378.
- Foxlin, E. (1996). "Inertial Head-Tracker Sensor Fusion by a Complementary Separate-Bias Kalman Filter," *Proceedings of VRAIS '96*, IEEE, pp. 185-194.
- Frey, W. (1996). *Application of Inertial Sensors and Flux-Gate Magnetometers to Real-Time Human Body Motion Capture*, Master's Thesis, Naval Postgraduate School, Monterey, CA.
- Fuchs, E. (1993). *Inertial Head-Tracking*, Master's Thesis, Massachusetts Institute of Technology, Cambridge MA.
- Funda, J., Taylor, R., & Paul, R. (1990). "On Homogeneous Transforms, Quaternions, and Computational Efficiency," *IEEE Transactions on Robotics and Automation*, Vol. 6, No. 3, pp. 382-388.
- Haas Automation, Inc. (1992) *Haas Model: TRT-7 Tilting Rotary Table*, Chatsworth, CA.
- Harris, G., & Smith, P. (Eds.) (1996). *Human Motion Analysis, Current Applications and Future Directions*, IEEE Press, Piscataway, New Jersey.
- Honeywell Inc. (1998). *Honeywell Three-Axis Magnetic Sensor Hybrid, HMC2003*.
- IntegriNautics Corporation. (2000). Private communication with development engineer. Menlo Park, CA 94025.
- Koozekanani, S., Barin, K., McGhee, R., & Chang, H. (1983). "A Recursive Free-Body Approach to Computer Simulation of Human Postural Dynamics", *IEEE Transactions on Biomedical Engineering*, Vol. BME-30, No. 12, pp. 787-792.
- Livingston, M. & State A. (1997) "Magnetic Tracker Calibration for Improved Augmented Reality Registration", *Presence: Teleoperators and Virtual Environments*, Vol. 6, No. 5, pp. 532-546.

McGhee, R., Bachmann, E., Yun X. & Zyda, M. (2000a). "Real-Time Tracking and Display of Human Limb Segment Motions Using Sourceless Sensors and a Quaternion-Based Filtering Algorithm - Part I: Theory," MOVES Academic Group Technical Report NPS-MV-01-001, Naval Postgraduate School, Monterey, CA. <http://npsnet.org/~moves/TechReports/NPS-MV-01-001.pdf>

McGhee, R., Bachmann, E., Brutzman, D., & Zyda, M. (2000b) "Rigid Body Dynamics, Inertial Reference Frames, and Graphics Coordinate Systems: A Resolution of Conflicting Conventions and Terminology," MOVES Academic Group Technical Report NPS-MV-01-002, Naval Postgraduate School, Monterey, CA.

McGhee, R., Nakano, E., Koyachi, N., & Acachi, H. (1986). "An Approach to Computer Coordination of Motion for Energy-Efficient Walking Machines," *Bulletin of Mechanical Engineering Laboratory, Japan*, No. 43.

McKinney, D. (2000). McKinney Technology, 9 Glen Avenue, Prunedale, CA, 93907, doug@mt.to .

Meyer, K., Applewhite, H., & Biocca, F. (1992). "A Survey of Position Trackers," *Presence: Teleoperators and Virtual Environments*, Vol. 1, No. 2, pp. 173-200.

Molet, T., Boulic R., & Thalmann D. (1999A). "Human Motion Capture Driven by Orientation Measurements," *Presence: Teleoperators and Virtual Environments*, Vol. 8, No. 2, MIT Press, Cambridge MA, pp. 187-203.

Molet, T., Aubel, A., Tolga, C., Carion, S., Lee, E., Naagnenat-Thalmann, N., Hoser, H., Pandzic, I., Sannier, G., & Thalmann, D. (1999b). "Anyone for Tennis," *Presence: Teleoperators and Virtual Environments*, Vol. 8, No. 2, MIT Press, Cambridge MA., pp. 140-156.

Molet, T., Boulic R., & Thalmann D, (1999a). "Human Motion Capture Driven by Orientation Measurements," *Presence: Teleoperators and Virtual Environments*, Vol. 8, No. 2, MIT Press, Cambridge MA, pp. 187-203.

Nixon, M., McCallum, B., Fright, W., & Price, N. (1998). "The effects of Metals and Interfering Fields on Electromagnetic Trackers," *Presence: Teleoperators and Virtual Environments*, Vol. 7, No. 2, MIT Press, Cambridge, MA, pp. 204-218.

Skopowski, P. (1996). Immersive Articulation of the Human Upper Body in a Virtual Environment, Master's Thesis, Naval Postgraduate School, Monterey, CA.

Token American Inc. (1998). *Token CG16D Solid State Rate Sensor Data Sheet*, http://www.token.com/Token_America_Products/46/p46c/p46c.html

Usta, U. (1999). Comparison of Quaternion and Euler Angle Methods for Joint Angle Animation of Human Figure Models, Master's Thesis, Naval Postgraduate School, Monterey, CA.

Welch, G., Bishop, G., Vicci, L., Brumback, S., Keller, L., & Colucci, D. (1999) “The HiBall Tracker: High-Performance Wide-Area Tracking for Virtual and Augmented Environments,” *Proceedings of the ACM Symposium on Virtual Reality Software and Technology 1999 (VRST 99)*, University College, London.

Yun, X., Bachmann, E., McGhee R., Whalen, R., Roberts, R., Knapp, R., Healey, A., & Zyda M. (1999). “Testing and Evaluation of an Integrated GPS/INS System for Small AUV Navigation,” *IEEE Journal of Ocean Engineering*, Vol. 24, No. 3, pp. 396-404.

Appendix A: Implementation of the Quaternion Attitude Filter Algorithm

The implemented calculations in the numbered procedural blocks of Figure 5 are given below. A complete theoretical discussion is available in (McGhee et al., 2000a). Steps 1 through 6 are completed only when calculating a new drift correction.

1. Calculate Estimation Error:

The gravitational and magnetic reference vectors are transformed to body coordinates by the following quaternion transformations and then normalized to unit length

$$\hat{h} = q^* \otimes m \otimes q \quad (13)$$

$$\hat{b} = q^* \otimes n \otimes q \quad (14)$$

where m and n are pure quaternions respectively expressing the gravity and local magnetic field vectors in Earth-fixed coordinates.

The accelerometer and magnetic errors in quaternion form are computed separately as follows

$$h - \hat{h} \quad (15)$$

$$b - \hat{b} \quad (16)$$

where h and b are pure quaternions respectively expressing measured gravity and local magnetic field vectors in a body-fixed coordinates frame.

If differential weighting is being applied, the magnetic error is computed as

$$\rho(b - \hat{b}) \quad (17)$$

where ρ is the differential weighting factor.

Combining the vector portions of the accelerometer and magnetometer errors creates the 6 x 1 error vector.

$$\bar{\varepsilon}(\hat{q}) = \begin{bmatrix} h - \hat{h} \\ b - \hat{b} \end{bmatrix} \text{ or } \begin{bmatrix} h - \hat{h} \\ \rho(b - \hat{b}) \end{bmatrix} \quad (18)$$

The criterion error function may be calculated at this point as

$$\varphi(\hat{q}) = \bar{\varepsilon}^T(\hat{q}) \bar{\varepsilon}(\hat{q}) \quad (19)$$

2. Calculate X Matrix:

The columns of the 6 x 4 X matrix is formed by taking the partial derivatives of the error vector with respect to each of the four components of \hat{q} . The real or scalar part of each quaternion is discarded.

The transpose of the implemented X matrix is calculated as

$$X^T = \begin{bmatrix} ((1 \otimes m) \otimes \hat{q}) + (\hat{q}^{-1} \otimes (m \otimes 1)) & ((1 \otimes n) \otimes \hat{q}) + (\hat{q}^{-1} \otimes (n \otimes 1)) \\ ((-i \otimes m) \otimes \hat{q}) + (\hat{q}^{-1} \otimes (m \otimes i)) & ((-i \otimes n) \otimes \hat{q}) + (\hat{q}^{-1} \otimes (n \otimes i)) \\ ((-j \otimes m) \otimes \hat{q}) + (\hat{q}^{-1} \otimes (m \otimes j)) & ((-j \otimes n) \otimes \hat{q}) + (\hat{q}^{-1} \otimes (n \otimes j)) \\ ((-k \otimes m) \otimes \hat{q}) + (\hat{q}^{-1} \otimes (m \otimes k)) & ((-k \otimes n) \otimes \hat{q}) + (\hat{q}^{-1} \otimes (n \otimes k)) \end{bmatrix} \quad (20)$$

where $\hat{q}^{-1} = \hat{q}^*$ if \hat{q} is of unit length and

$$1 = \begin{bmatrix} 1 \\ 0 \\ 0 \\ 0 \end{bmatrix}, \quad i = \begin{bmatrix} 0 \\ 1 \\ 0 \\ 0 \end{bmatrix}, \quad j = \begin{bmatrix} 0 \\ 0 \\ 1 \\ 0 \end{bmatrix}, \quad k = \begin{bmatrix} 0 \\ 0 \\ 0 \\ 1 \end{bmatrix} \quad (21)$$

3. Calculate X_v Matrix:

The transpose of the 6 x 3 X_v matrix is calculated as follows.

$$X_v^T = \begin{bmatrix} X(\hat{q} \otimes i)^T \\ X(\hat{q} \otimes j)^T \\ X(\hat{q} \otimes k)^T \end{bmatrix} \quad (22)$$

4. Calculate full Delta v step:

The 3 x 1 Δv_{full} vector is given by

$$\Delta v_{full} = (X_v^T X_v)^{-1} X_v \bar{\epsilon}(\hat{q}) \quad (23)$$

The inverse is calculated using Gaussian elimination.

5. Calculate full Delta q step:

The vector Δv_{full} is used as the imaginary part of a pure quaternion to calculate 4 x 1 correction vector, Δq_{full} .

$$\Delta q_{full} = \hat{q} \otimes (0, \Delta v_{full}) \quad (24)$$

6. Calculate q-dot epsilon:

The filter gain, k , is applied to produce the scaled correction step.

$$\dot{q}_\varepsilon = k \Delta q_{full} \quad (25)$$

7. Derive Rate Quaternion, q-dot:

The rate quaternion is calculated using the rotational rates about the x , y , and z body-axes.

$$\dot{q} = \frac{1}{2} \hat{q} \otimes (0 \quad p \quad q \quad r) = \frac{1}{2} \hat{q} \otimes {}^B \omega \quad (26)$$

8. Estimate Orientation, q-hat:

The updated orientation estimate (new \hat{q}) is calculated through Euler integration and then normalized to unit length to avoid truncation and round-off errors.

$$\hat{q} + \Delta t (\dot{q} + \dot{q}_\varepsilon) \quad (27)$$

Appendix B: MARG Sensor Calibration Algorithm Procedure

Finding Inertial Sensor Null Points and Scale Factors

1. Place the sensor in a stationary position on a flat level nonmagnetic surface with the positive z -axis of the sensor pointing down. While the sensor is in this position record the maximum voltage reading for the z -axis accelerometer as $accZMax$. Set the rate sensor null points $angXNull$, $angYNull$ and $angZNull$ to the rate sensor readings obtained while in this stationary position.
2. Rotate the sensor 90 degrees about the positive x -axis. While performing this rotation integrate the output of the x -axis rate sensor
3. Following completion of the rotation, record the maximum voltage reading for the y -axis accelerometer as $accYMax$. Make a first estimate of the x -axis rate sensor scale factor, $angScaleXOne$, using Eq. (5).
4. Rotate the sensor 180 degrees about the negative x -axis. While performing this rotation integrate the output of the x -axis rate sensor.
5. Following completion of the rotation, record the minimum voltage reading for the y -axis accelerometer as $accYMin$. Make a second estimate of the x -axis rate sensor scale factor, $angScaleXTwo$, using Eq. (5). Set the scale factor for the x -axis rate sensor to the average of $angScaleXOne$ and $angScaleXTwo$. Calculate the null point for the y -axis accelerometer using Eq. (1).
6. Rotate the sensor 90 degrees about the positive z -axis. While performing this rotation integrate the output of the z -axis rate sensor.
7. Following completion of the rotation, record the minimum voltage reading for the x -axis accelerometer as $accXMin$. Make a first estimate of the z -axis rate sensor scale factor, $angScaleZOne$, using Eq. (5).
8. Rotate the sensor 180 degrees about the negative z -axis. While performing this rotation integrate the output of the z -axis rate sensor.
9. Following completion of the rotation, record the maximum voltage reading for the x -axis accelerometer as $accXMax$. Make a second estimate of the z -axis rate sensor scale factor, $angScaleZTwo$, using Eq. (5). Set the scale factor for the z -

- axis rate sensor to the average of *angScaleZOne* and *angScaleZTwo*. Calculate the null point for the x-axis accelerometer using Eq. (1).
10. Rotate the sensor 90 degrees about the negative y-axis. While performing this rotation integrate the output of the y-axis rate sensor.
 11. Following completion of the rotation, record the minimum voltage reading for the z-axis accelerometer as *accZMin*. Make a first estimate of the y-axis rate sensor scale factor, *angScaleYOne*, using Eq. (5). Calculate the null point for the z-axis accelerometer using Eq. (1).
 12. Rotate the sensor 180 degrees about the positive y-axis. While performing this rotation integrate the output of the y-axis rate sensor.
 13. Following completion of the rotation, make a second estimate of the y-axis rate sensor scale factor, *angScaleYTwo*, using Eq. (5). Set the scale factor for the y-axis rate sensor to the average of *angScaleYOne* and *angScaleYTwo*.
 14. Calculate the accelerometer scale factors using Eq. (2).

Finding Magnetometer Maximum and Minimum Voltage Readings

15. Point the sensor x-axis north and rotate the sensor 360 degrees about the y-axis. Record the minimum and maximum voltages obtained from the x-axis magnetometer during this rotation.
16. Point the sensor y-axis north and rotate the sensor 360 degrees about the x-axis. Record the minimum and maximum voltages obtained from the y-axis and z-axis magnetometers during this rotation.
17. Calculate the magnetometer null points using Eq. (3). Calculate the magnetometer scale factors using Eq. (4).

Finding Gravity and Magnetic Reference Vectors

18. Place the sensor in the reference position with the positive x-axis pointing toward magnetic north, positive y-axis east, and the positive z-axis pointing down. While in this stationary position record the reading produced by the magnetometers and accelerometers. The six numbers produced correspond to the x, y, and z components of the two reference vectors.

INITIAL DISTRIBUTION LIST

1. Defense Technical Information Center 2
8725 John J. Kingman Rd., STE 0944
Ft. Belvoir, VA 22060-6218
2. Dudley Knox Library, Code 013 2
Naval Postgraduate School
Monterey, CA 93943-5100
3. Research Office, Code 09 1
Naval Postgraduate School
Monterey, CA 93943-5138